Possible Pb isotopic heterogeneity in chalcopyrite and magnetite - implications for Pb-Pb step-leaching chronology

[1,2]K.Bassano, [1,2]J. Hergt, [1,2]R. Maas & [1]J. Woodhead
[1]University of Melbourne, [2]pmd*CRC

INTRODUCTION

Pb-Pb step-leaching (PbSL) is a geochronological tool aimed at unmixing the common and radiogenic Pb components present in low-U minerals, using sequential leaching with a range of acids (HBr, HCl, HNO3, HF). Frei & Kamber (1995) showed that this approach can produce highly correlated Pb isotope unmixing arrays with age significance for a number of low-U silicate minerals, and thus provide a new single mineral dating tool for assemblages normally unfavourable for U-Pb dating. Studies on titanite suggest that Pb isotopic unmixing involves two main processes: (1) surface/crystallographic site dependent hydrolysis of metal cations; (2) progressive mobilisation of Pb isotope components from the leached gel-like structure. Radiogenic Pb is removed more slowly during progressive leaching, resulting in an effective separation of common and radiogenic Pb in sequential leach steps (Frei *et al*., 1997). Other potential mechanisms to produce linear isotope arrays during step leaching include selective Pb removal from high- and low-U domains in strongly zoned minerals, admixture of radiogenic Pb from U-rich impurities trapped during host mineral formation (e.g. monazite, zircon) or post-crystallization contamination along cracks, surfaces and cleavage planes. Obviously, interpretation of PbSL "ages" strongly depends on which of these processes is involved in a particular case.

Here we present the results of a laser ablation Pb isotope study of Proterozoic chalcopyrite and magnetite, with the aim of documenting the distribution of radiogenic vs. common Pb in these minerals. Laser ablation is an ideal tool to examine if Pb isotopes are distributed uniformly (suggesting uniform distribution of U in the mineral lattice) or in "hot spots" of localized U enrichment, such as in inclusions or cracks. This work is part of a wider study into the utility of PbSL for ore mineral geochronology.

SOLUTION BASED PbSL AND TRACE ELEMENT DISTRIBUTION

Conventional (chemical) PbSL on Cu sulphides and magnetite from several Proterozoic hydrothermal base metal deposits performed in this study typically produced strongly scattered data in $^{206}Pb/^{204}Pb$ vs. $^{207}Pb/^{204}Pb$ space (Fig. 1). Formal isochron regressions consequently yield large MSWD values and "age" errors. Apparent ages are either similar to, or younger than, known mineral formation ages (typically 1.1-1.35 *vs.* 1.5-1.6 Ga based on common Pb model or monazite U-Pb chronologies).

Bulk trace element patterns for multiple aliquots of each sample were obtained to assess if isotopic scatter in PbSL plots was reflected in trace element distributions. For example, heterogeneously distributed U-rich inclusions, or the presence of exotic U-Pb-rich impurities on cracks or surfaces of the host mineral, would be expected to result in variable trace element patterns from grain to grain. The same is true if Pb isotope variability is the result of heterogeneously distributed U and/or open system behaviour. On the other hand, homogeneous trace element patterns in multiple aliquots would suggest rather uniform intrinsic U (and thus Pb isotope) distribution. Scatter in PbSL patterns might thus merely be an artefact of the leaching process.

Our results indicate that trace element patterns are generally reproducible. However, some samples show notable variations in U concentrations (Fig. 2). These samples were selected for *in situ* LA-ICPMS analysis to determine if heterogeneous bulk U distribution is reflected in Pb isotope heterogeneity at a sub-grain scale.

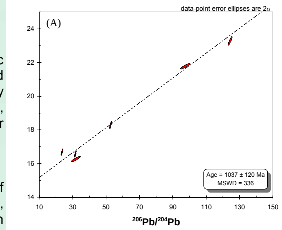

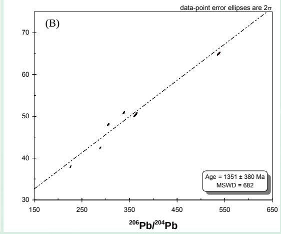

Figure 1: Solution-based PbSL arrays for (a) Copper Blow magnetite (error ellipses exaggerated 4x) and (b) Ernest Henry chalcopyrite. Note large scatter and imprecise "ages".

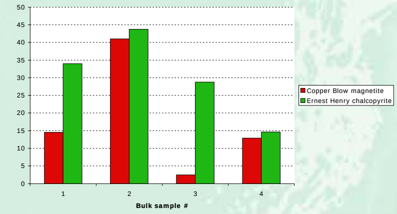

Figure 2: Variation of U content in multiple (c.20 mg) aliquots (4 each) of Ernest Henry chalcopyrite and Copper Blow magnetite. U in the chalcopyrite varies by c 2.5x while the magnetite shows a much larger (c 20x) variation.

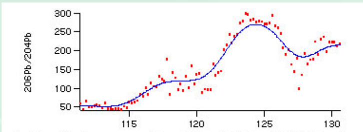

Figure 3: Time-resolved laser-ablation $^{206}Pb/^{204}Pb$ ratios for part of a line scan on Ernest Henry chalcopyrite. The peak near ~120 sec may reflect a U-rich inclusion. Smooth line is visual fit.

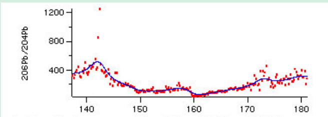

Figure 4: Time-resolved laser-ablation $^{206}Pb/^{204}Pb$ ratios for part of a line scan on Ernest Henry chalcopyrite.

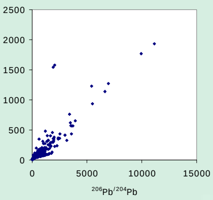

Figure 5: Laser-ablation Pb isotope results for Ernest Henry chalcopyrite. Each data point shown represents the average of a short linear ablation track or of a discrete segment (of approx. constant Pb isotope ratios) from the long traverse.

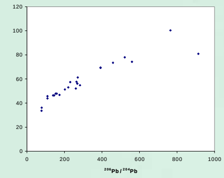

Fig.6 Laser-ablation Pb isotope data for long traverse on Ernest Henry chalcopyrite. All 0.2 sec integrations are shown, illustrating the enormous range in Pb isotope ratios. Note that very drastic changes in signal size associated with large spikes will lead to spurious recovery effects in the Faraday detector amplifier circuitry. The position of the most radiogenic points (spikes) may thus be an analytical artefact.

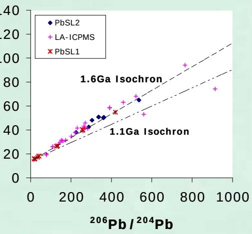

Figure 7: Laser-ablation Pb isotope data for long traverse on Ernest Henry chalcopyrite (data with $^{206}Pb/^{204}Pb$ >1000 omitted). Also shown are results for 2 PbSL experiments of same sample. Dispersion of laser ablation results helps explain scatter in PbSL data.

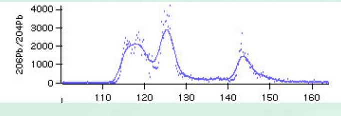

Figure 8: Time-resolved $^{206}Pb/^{204}Pb$ trace for linear scan across surface of Copper Blow magnetite.

LASER ABLATION ICP-MS

In situ Pb isotope ratios were determined using the methods of Paul *et al*. (2005). Data were obtained from linear traverses of variable length on polished mineral surfaces. Analytical precision for the present study is thus difficult to quantify. It is probably <10% (2 sigma for $^{206}Pb/^{204}Pb$), but >>10% where signals were close to detection limits.

Ernest Henry Chalcopyrite

Short line scans and one longer whole-crystal traverse indicate a high degree of isotopic heterogeneity in this chalcopyrite, with $^{206}Pb/^{204}Pb$; ranging from <50 to >10000 (Fig.6). Time-resolved plots of two short line scans are shown in Figs. 3 and 4. The $^{206}Pb/^{204}Pb$ maximum near 125 secs (Fig.3) may be related to an inclusion, and a very short-lived spike to even higher $^{206}Pb/^{204}Pb$ is evident in Fig.4.

Inspection of chalcopyrite surfaces after ablation suggests that some of the excursions to high $^{206}Pb/^{204}Pb$ are indeed associated with inclusions, crystal boundaries and micro-cracks, implying a complex mix of Pb isotope sources in the sulphide. Radiogenic Pb from such sites may diffuse into the host mineral, for example creating the relatively broad high-^{206}Pb peak shown in Fig.3. Accumulation of radiogenic Pb in annealed cracks and on grain boundaries has been documented for Bushveld Complex sulphides. (Mathez and Waight, 2003). In addition to the short-lived spikes and humps produced by inclusions and crack-held Pb, the presence of plateaus with roughly constant $^{206}Pb/^{204}Pb$ in the laser ablation traverses suggests that true U zoning in the sulphide may also contribute to the Pb isotopic variation.

Pb-Pb isotope diagrams illustrate the complex nature of the chalcopyrite data. In Fig.5, the averages for the short linear traverses and for segments of the long traverse define a roughly linear array close to a 1.5-1.6 Ga reference isochron. By contrast, a subset of the data defines a shallower trend close to a c. 1.1 Ga reference isochron. In Fig.7, data from the long traverse have not been averaged, and all 0.2 sec integrations are shown. Overall, the data again do not define a single trend, and $^{207}Pb/^{206}Pb$ ratios for the most radiogenic points (from extreme spikes associated with very small, very U-rich inclusions) are too high to lie on the 1.6 Ga reference isochron. However, the less radiogenic points within the main cluster in Fig.6 do plot close to 1.5-1.6 Ga reference lines (Fig.7). The PbSL data for the same sample are broadly collinear with the laser-ablation data (Fig.7). The larger dispersion of the laser ablation data, in particular the data points with low $^{207}Pb/^{206}Pb$ (well below the 1.6 Ga reference line) illustrates the Pb isotopic heterogeneity within the chalcopyrite and explains the scatter in the data.

Copper Blow Magnetite

PbSL ages for this sample are some 400 Ma too young, suggesting U addition at some stage long after original mineral formation. Laser-ablation patterns show considerable structure, with strong spikes to $^{206}Pb/^{204}Pb$ > 4000 superimposed on a background that is close to or at the detection limit of the Faraday detectors. Spikes develop rapidly but decay more slowly with enhanced uranogenic Pb isotope ratios for considerable periods.

On a plot of $^{208}Pb/^{206}Pb$ vs. $^{207}Pb/^{206}Pb$, the magnetite data define two separate but roughly collinear clusters (Fig.9). The cluster centred on $^{208}Pb/^{206}Pb$≈2 is common Pb while the cluster at low $^{208}Pb/^{206}Pb$ is variably radiogenic Pb. At $^{208}Pb/^{206}Pb$ =0, the $^{207}Pb/^{206}Pb$ is ≈0.08, i.e. radiogenic Pb with a model age near 1200 Ma. This is similar to the PbSL age for this magnetite. The large amount of scatter reflects the small signal intensities for the background, and possibly fast signal change effects on Faraday detectors (see above) for the radiogenic cluster. Nevertheless, the overall pattern is clear: U-rich, low-Th inclusions c.1200 Ma old contribute the bulk of radiogenic Pb in this sample, and this controls the PbSL pattern. The apparent co-linearity between the two clusters in Fig 9 suggests that only one radiogenic Pb component (1200 Ma old) exists in this sample. Radiogenic Pb generated from ≈1.6 Ga would have a distinctly higher $^{207}Pb/^{206}Pb$ (near 0.1) not obvious in Fig.9. Assuming that the magnetite originally formed near 1.6 Ga or earlier, it appears to have formed with low U/Pb. Several 100 Ma later, a U-rich but Th-poor component was added and distributed within the magnetite in the form of discrete inclusions, perhaps in a manner analogous to secondary fluid inclusions which often line healed fractures in the host mineral

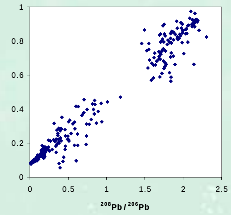

Figure 9: $^{207}Pb/^{206}Pb$ vs. $^{208}Pb/^{206}Pb$. Laser-ablation data for linear scans on Copper Blow magnetite, all 0.2 sec integrations shown. Upper cluster shows common Pb compositions with $^{207}Pb/^{206}Pb$ near 1 and $^{208}Pb/^{206}Pb$ near 2). Second cluster incorporates variably radiogenic compositions culminating in essentially purely radiogenic ($^{208}Pb/^{206}Pb$ near 0, i.e. no thorogenic Pb) with $^{207}Pb/^{206}Pb$ ≈0.08, equivalent to a model age near 1200 Ma.

CONCLUSIONS

Laser-ablation Pb isotope data for hydrothermal chalcopyrite and magnetite with heterogeneous U distributions at the grain-to-grain scale reveal:

1. Strong and variable Pb isotopic structure at the sub-mm scale.
2. ^{206}Pb-rich spikes and humps related to U-rich inclusions and/or impurities along grain surfaces and cracks
3. Ernest Henry chalcopyrite shows a dominant, c. 1.6 Ga radiogenic component, most likely carried in inclusions. Data related to this component are collinear with PbSL arrays. A second minor radiogenic component with lower $^{207}Pb/^{206}Pb$ may explain scatter in PbSL patterns to younger ages.
4. Copper Blow magnetite contains clear evidence for U-rich (low-Th/U) micro-inclusions c 1200 Ma old. Older radiogenic Pb appears to be absent.
5. Both deposits were affected by an event that introduced U near 1.2-1.1 Ga.
6. Strongly scattered PbSL patterns with anomalously young apparent ages for these minerals result from mixing of at least 2 radiogenic Pb components (Ernest Henry chalcopyrite), or from mixing of common Pb with a heterogeneous radiogenic Pb component related to late addition of U (Copper Blow magnetite).

predictive mineral discovery
Cooperative Research Centre

REFERENCES

Cherney S., Cook J.M., Styles M., and Cameron E.M. (1995) Determination of the three-dimensional distributions of precious metals by laser ablation microprobe-inductively coupled plasma-mass spectrometry (LAMP-ICP-MS). Chemical Geology, 124, 55-65.
Frei, R. and Kamber, B. S. (1995). Single mineral Pb-Pb dating. *Earth and Planetary Science Letters*, 129, pp. 261-268.
Paul B., Woodhead J.D., and Hergt J. (2005) Improved in situ isotope analysis of low-Pb materials using LA-MC-ICP-MS with parallel ion counter and Faraday detection. *Journal of Analytical and Atomic Spectrometry*, 20, 1350-1357.

Kate Bassano
School of Earth Sciences / pmd*CRC
The University of Melbourne
Parkville 3010 VIC

Phone: (03) 8344 9669
Email:k.bassano@pgrad.unimelb.edu.au
www.pmdcrc.com.au